

## Diffusion mechanisms taking place at the early stages of cobalt deposition on Au(111)

This article has been downloaded from IOPscience. Please scroll down to see the full text article.

2008 J. Phys.: Condens. Matter 20 265010

(<http://iopscience.iop.org/0953-8984/20/26/265010>)

View [the table of contents for this issue](#), or go to the [journal homepage](#) for more

Download details:

IP Address: 129.252.86.83

The article was downloaded on 29/05/2010 at 13:18

Please note that [terms and conditions apply](#).

# Diffusion mechanisms taking place at the early stages of cobalt deposition on Au(111)

O A Oviedo, E P M Leiva and M M Mariscal

Unidad de Matemática y Física, Facultad de Ciencias Químicas, Universidad Nacional de Córdoba, INFIQC, (5000) Córdoba, Argentina

E-mail: [marcelo.mariscal@gmail.com](mailto:marcelo.mariscal@gmail.com)


Received 12 February 2008, in final form 25 April 2008

Published 28 May 2008

Online at [stacks.iop.org/JPhysCM/20/265010](http://stacks.iop.org/JPhysCM/20/265010)

## Abstract

In the present work a detailed atomic-level analysis of some of the main diffusion mechanisms which take place during cobalt adatom deposition are studied within atom dynamics (AD) and the nudged elastic band (NEB) method. Our computer simulations reveal a very fast exchange between Co and Au atoms when the deposit is a single cobalt adatom. However, when the nucleus size increases, a decrease in the exchange probability is observed. Activation energies for different transitions are obtained using AD in combination with the NEB method.

 This article features online multimedia enhancements available from [stacks.iop.org/JPhysCM/20/265010](http://stacks.iop.org/JPhysCM/20/265010)

(Some figures in this article are in colour only in the electronic version)

## 1. Introduction

The understanding of atomic diffusion mechanisms on surfaces is an interesting topic because of its key importance in crystal growth, heterogeneous catalysis, phase transitions, segregation and surface patterning at the nanometer scale. For the last 50 years researchers have approached the problem through theoretical models and, whenever possible, through sophisticated experiments [1]. Recently, Labayan and colleagues [2] have revealed the atomic mechanisms underlying the apparent collective motion of long strings of hexagonally arranged Au atoms embedded into the first atomic plane of Au(100). Using video-STM they were able to record 10–20 images per second, a considerably large number compared with the 30–200 s required to capture a single image with conventional STM. Due to this limitation to obtaining experimental evidence of dynamics of atomic transport on surfaces, atomistic computer experiments assume great importance.

The Co/Au system has been the subject of many experiments mainly because of the potential properties that could be expected from the combination of a ferromagnetic material with a noncorrosive substrate one. Although several deposition studies for Co on single-crystal substrates have been

performed in UHV conditions [3–7], only a few reports have been found in the literature dealing with the morphology of thin electrochemically growth Co films on Au surfaces [8, 9].

Thermally activated diffusion of adatoms on fcc metal surfaces may take place either by a hopping mechanism (an adatom hopping between adjacent sites) or via an exchange mechanism [10, 11] (an adatom exchange with one or several surface atoms). Different theoretical approaches can be adopted to study surface diffusion processes: density functional calculations (DFT), for instance, can be employed with a limited number of atoms (ca. 150) which, in some cases, may be insufficient to describe exchange processes. Another type of approximation uses semiempirical many-body potentials, which can be used to treat a large number of particles (up to millions) [12–14].

In particular, self-diffusion processes have been studied by Feibelman [15] for fcc(100) surfaces within the DFT formalism. Feibelman [15] found that hopping diffusion takes place on the fcc(100) surfaces of the 4d metals, whereas the exchange mechanism is favored for the same surfaces of the 5d metals. Semiempirical calculations using the embedded-atom method (EAM) [16] and the Rosato–Guillope–Legrand (RGL) potential [17] were performed for fcc(100), (110) and (111) surfaces; however, only hopping diffusion was

considered in that case. EAM in combination with the dimer method has been used by Henkelman *et al* [18] to study the exchange mechanism in self-diffusion of Al(100), in very good agreement with Feibelman's results [15].

Exchange diffusion studies on fcc(111) metal surfaces have been performed by means of the second-moment approximation of tight-binding theory (SMTB) [19]. Atom dynamics simulation in combination with the NEB method [20, 21] was used to calculate diffusion barriers of the homoatomic systems Au, Cu, Ni, Pt and the heteroatomic ones Co/Pt(111) and Co/Au(111) [19]. However, only single adatom diffusion was considered, and the effect of the adsorbate–adsorbate interaction was not examined in that work. *Ab initio* calculations for fcc(111) exchange diffusion are less frequent mainly due to the large number of atoms involved in the whole process.

Surface diffusion of single Co adatoms as well nucleation and growth of Co clusters on Au(111) reconstructed surfaces have been studied by Bolou and coworkers [22] using the many-body semiempirical potential second-moment tight-binding model (SMTB). The aim of the present work is to elucidate the atomistic mechanisms during deposition of a single, a dimer and a trimer of cobalt atoms on an Au(111) surface. For a single Co adatom on the unreconstructed and on the herringbone reconstructed surface of Au(111), the main diffusion pathway has been reported to be hopping [22, 23]. Our nudged elastic band calculations show that, for the present parameterization, too high activation energies may result if a relatively small number of atoms are relaxed. On the other hand, adsorbate–adsorbate interactions are considered for the case of small Co nuclei on Au(111) unreconstructed surfaces. In a previous work [24] one of us suggested that, when the number of Co adatoms arriving at the surface is large enough, i.e. 3–6 atoms, the diffusion mechanism can change from exchange to hopping due to the strong Co–Co interaction. As a first attempt, and because of the very short times involved in the single-exchange process, atom dynamics (AD) simulations were performed in the present work to study single Co atom diffusion. In multiple-exchange processes, the timescale reachable by AD was not enough to monitor diffusion at 300 K. Thus, a higher-temperature AD simulation was employed. With the structural information gathered from these simulations, NEB [20, 21] calculations were performed in order to get the minimum energy paths and an atomic-level description of the whole exchange process. From the AD simulations, waiting times, temperature and possible escape paths were obtained. Furthermore, activation energies and the minimum energy paths were obtained from the NEB calculations.

## 2. Calculation details

The primary objective of the present work was to determine the main diffusion pathways involved during the deposition of single, dimers and trimers of Co adatoms on the Au(111) surface. To reveal such mechanisms we performed canonical ( $NVT$ ) atom dynamics (AD) simulations at different temperatures (between 300 and 800 K). The Nordsieck fifth-order predictor–corrector [25] was used to integrate Newton's

equation of motion, with a time step of 2 fs. The metal surface, Au(111), was modeled as a slab of seven layers of atoms arranged on an fcc(111) lattice with 200 atoms per layer. The three bottom layers were held fixed and thus they mimicked the metal bulk effect. All atoms interacted through potentials calculated by the embedded-atom method, which takes into account many-body effects, characteristic of the metallic bond [26], as follows:

$$E_i = F(\rho_i) + \frac{1}{2} \sum \phi(r_{ij}). \quad (1)$$

The energy of atom  $i$ ,  $E_i$ , due to the surrounding atoms is assumed to consist of two parts, a two-body interaction  $\phi(r_{ij})$  and an embedding term  $F$  which depends on the local electron density  $\rho_i$ . The two-body term for dissimilar types of atoms is constructed following the analytical model of Johnson [27]:

$$\phi^{ab}(r) = \frac{1}{2} \left[ \frac{f^b(r)}{f^a(r)} \phi^{aa}(r) + \frac{f^a(r)}{f^b(r)} \phi^{bb}(r) \right] \quad (2)$$

where  $f^a(r)$  and  $f^b(r)$  are the single-atom electron densities at a distance  $r$  from an atom of type a or b, respectively, in the pure metal.

Periodic boundary conditions were applied in the  $[1\bar{1}2]$  and  $[110]$  directions. In the remaining discussion we refer to the  $z$  coordinate as that perpendicular to the substrate surface. For each system, a single atom, a dimer or a trimer of Co adatoms were alternately positioned on hollow fcc sites of the Au(111) surface. Subsequently, an AD run was performed, and the initial and final configurations were then used for the NEB calculations [20, 21] in order to obtain the activation energies  $E_a$  (saddle point) for the diffusive processes.

The energy along the minimum energy path (MEP) is given as a function of a reaction coordinate (RC). In mathematical terms, we have defined the RC at image  $N + 1$  of the NEB chain as:

$$\text{RC} = \frac{\sqrt{\sum_{j=1}^{N-1} |\Delta \mathbf{l}_j|^2}}{\sqrt{\sum_{j=1}^{N_{\text{tot}}-1} |\Delta \mathbf{l}_j|^2}} \quad (3)$$

where  $\Delta \mathbf{l}_j$  is the vector joining images  $j$  and  $j + 1$ , and  $N_{\text{tot}}$  is the total number of images of the chain.

Several atomic configurations extracted from the AD simulations were employed to build the NEB image chain, using a quenching algorithm. The purpose of this procedure was to improve the starting point for the NEB minimization process, introducing a more realistic image chain than a simple interpolation between initial and final configurations. The number of images used to obtain the minimum energy path was adjusted according to the system. For instance, for single adatom diffusion, 25 images with a spring force of  $5.0 \text{ nN \AA}^{-1}$  were used, whereas in the case of trimer deposition, 135 images with a spring force of  $5.0 \text{ nN \AA}^{-1}$  were required.

## 3. Results

### 3.1. Single adatom deposition

A single cobalt atom was placed on a hollow (fcc) site of the Au(111) surface layer, and an AD simulation at 300 K

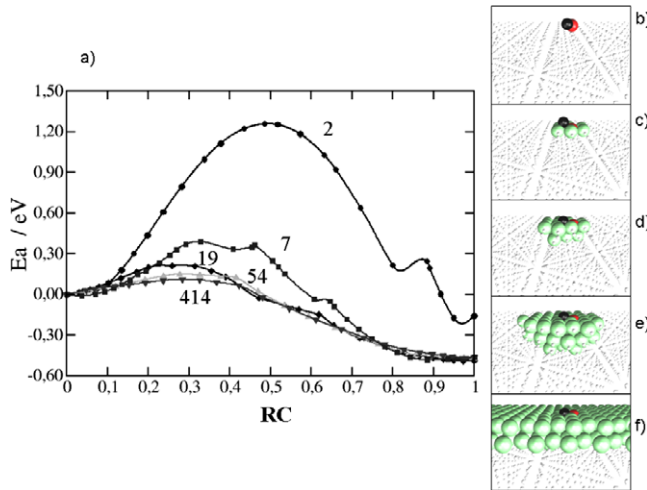


**Figure 1.** (a) Minimum energy path for single adatom exchange calculated with a different number of mobile atoms. (b)–(f) Atomic configurations showing the atoms allowed to relax during the NEB minimization.  $N = 2, 7, 19, 54$  and  $414$ , respectively.

was performed in order to relax the system. After 1 ps, the Co atom became embedded in the first surface layer, leading to a transient energetically unfavorable configuration, which resulted in the pull-out of the Au surface atom at 2 ps.

With the initial and final configurations determined from the AD simulation, NEB calculations were performed to acquire the minimum energy path for this exchange mechanism. The most relevant quantity obtained in this procedure is the activation energy of the process,  $E_a$ , which can be used in a proper kinetic scheme to obtain reaction rates. The NEB method was applied considering a different number of mobile atoms in the simulation cell, in order to test the convergence with respect to this parameter. Figure 1 shows the energy profile along the reaction coordinate RC for different numbers of mobile atoms. When only two neighboring atoms were allowed to relax, two activated processes were detected, the larger activation energy observed corresponding to 1.20 eV. As the number of neighbors allowed to relax was increased, i.e. when the first wrapping shell was considered, the  $E_a$  decreased to 0.20 eV and only one transition state was observed. Finally, using 414 mobile atoms, an  $E_a$  value of 0.11 eV was found. As can be observed, if only a few atoms are relaxed, the activation energies may be strongly overestimated. Bulou [19] have estimated an energy exchange for a single cobalt adatom on Au(111) of 0.536 eV using the second-moment approximation of tight-binding theory SMTB-NEB

calculations, a similar semiempirical many-body potential. Aside from the transition discussed above and found in our AD simulations, Bulou *et al* [19] have also reported a so-called medium-range transition. For this process we observed a converged activation energy of 0.27 eV.

All the calculations reported in the present paper were done for the fcc(111) lattice. However, on real Au(111) surfaces both fcc and hcp domains are present due to the surface reconstruction. Figure 1 showed the calculated barriers for the Co–Au exchange to occur to be rather sensitive to the number of atoms allowed to relax their positions so than one may expect that the behavior of Co adatoms at the finite fcc areas of the reconstructed Au(111) surface may be different from that on the (infinite) unreconstructed surface. However, figure 1 also shows that the barrier height for single adatom exchange can be calculated with a relatively good accuracy considering the relaxation of 54 atoms, a system that involves up to some third-nearest neighbors. Since the distances that separate hcp and fcc distances are larger than third-nearest-neighbor distances, we expect that our results, obtained for perfect flat surfaces (i.e. with fcc domains), are applicable to the fcc region of the reconstructed surface.

The analysis of the atomic configurations together with the energy profile contributes to the understanding of the diffusion mechanism. The whole exchange processes comprise two steps: the opening of the gold surface in the vicinity of the Co atom (activated process), simultaneously with the penetration of the cobalt atom, leading to the transition state or saddle point with the atomic configuration presented in figure 2(b). It is remarkable that no atoms protrude from the surface. The high compressive surface stress generated by the insertion of the Co atom is released by the later ejection of a gold atom, with a concomitant decrease of the potential energy of the system. Note also in figure 2(b) the high strain of the hexagon defined by the six nearest Au atoms on the surface around the exchange place.

### 3.2. Dimer adatom deposition

The second case studied involves the diffusion of a Co dimer into the Au(111) surface. This mechanism will be referred to as double short exchange (DSE) [19]. As in single atom deposition, atom dynamics simulations were performed in order to get the final configuration of the system required for the NEB calculations. In figure 3(a) a series of snapshots taken during the dynamic evolution of the system are shown. In frame (a) the initial state at  $t = 0$  with two cobalt adatoms

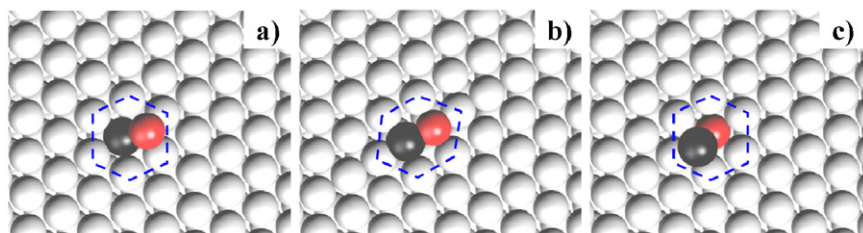


**Figure 2.** Atomic coordinates for single atom exchange at the initial state (a), saddle point (b) and final configuration after exchange (c) as calculated by NEB calculations. Note the strain of the surface in the vicinity of the Co atom marked by a hexagon. On-line: red sphere: Co atom, black: Au exchanged and gray: Au(111).

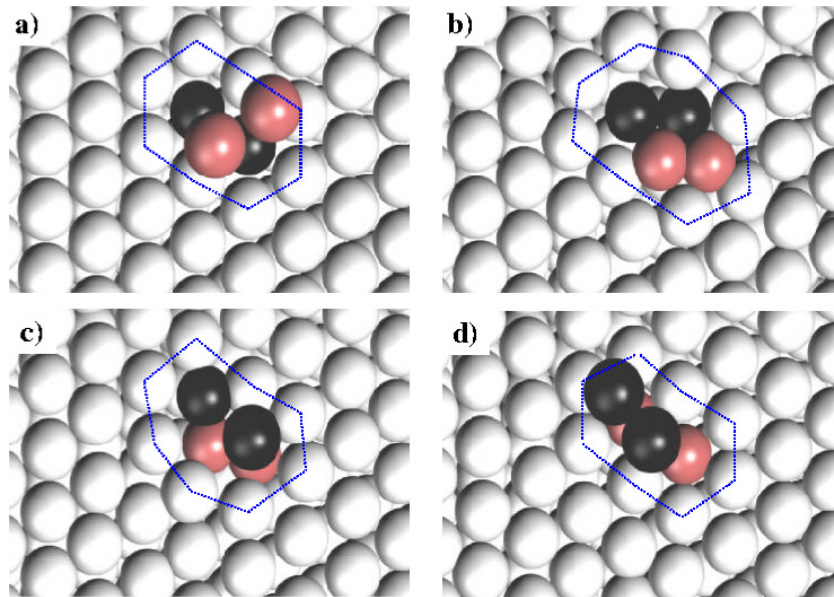


**Figure 3.** Snapshots taken from the atomic dynamics simulations of dimer exchange deposition at different times.  $t =$  (a) 0, (b) 6.6, (c) 7.8 and (d) 9.0 ps. Note the strain of the surface in the vicinity of the Co dimer marked by dotted lines. On-line: red sphere: Co atom, black: Au exchanged and gray: Au(111).

at the top surface is observed. In frame (b) an intermediate stage at  $t \approx 6.6$  ps, in which both Co atoms have been inserted into the topmost layer of the Au(111) surface, is shown. At  $t \approx 7.8$  ps the first Au atom appears on top of the surface layer (figure 3(c)). Subsequently at  $t = 9.0$  ps a second Au atom is expelled just beside the other one. In frame (d) the final configuration of the AD simulations is shown with the two gold atoms on top of the surface layer at their equilibrium positions. Again a very fast exchange between Co and Au atoms was observed by means of AD simulations. In this case a two-step concerted process takes place involving the insertion of two Co atoms and the subsequent expulsion of two Au atoms at different times.

In order to obtain the activation energy values involved in the whole process, the atomic coordinates of the system shown in figures 3(a) and (d) were used as initial and final states for the NEB calculations, respectively. Figure 4(a) displays the energy profile along the reaction coordinate RC for the DSE mechanism. As seen in the figure, an activation energy  $E_a = 0.18$  eV was obtained. The whole process can be more properly understood by splitting the energy profile into different regions. In the interval ( $0.0 < RC < 0.1$ ), a rearrangement of the surface atoms occurs, involving an activation energy  $E_a = 0.18$  eV, i.e. a surface opening is required to insert the first Co adatom. In the region between ( $0.1 < RC < 0.2$ ) a very small activation energy of  $E_a = 0.02$  eV is associated with the insertion of the first Co adatom into the first Au(111) layer. Afterward, between ( $0.2 < RC < 0.5$ ), the energy decreases steeply due to the expulsion of the first Au atom toward the surface. The insertion of the second Co atom is followed by a small change in the slope of the curve in figure 4(a), indicating that this process is not activated. In the region ( $0.5 < RC < 0.8$ ), the expulsion of a second Au atom occurs. This is also a non-activated process. At the end of the energy

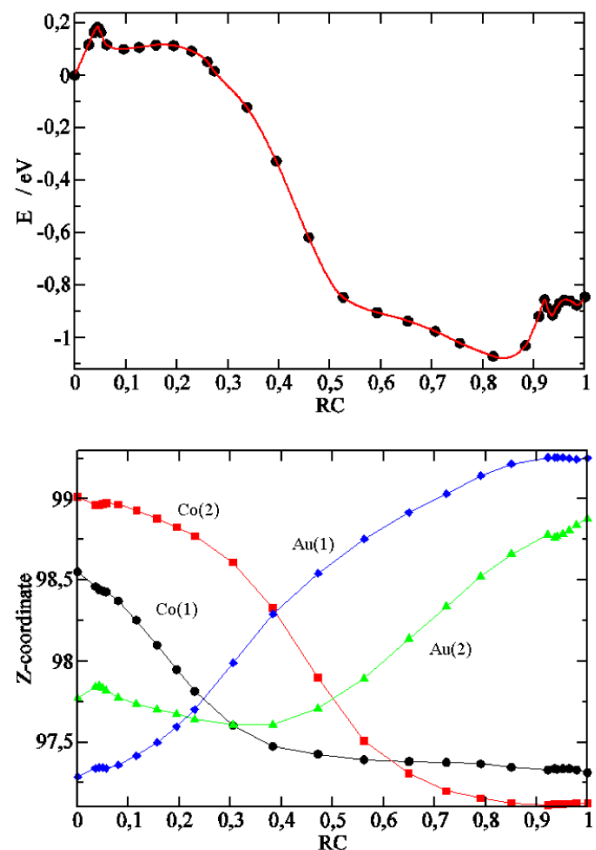


**Figure 4.** (a) Minimum energy path for dimer exchange deposition calculated with the NEB method. (b)  $z$  displacement of the atoms involved in the exchange of a Co dimer.

profile, ( $RC \approx 0.95$ ) a second activated process is found. This is related to the diffusion of the two Au adatoms approaching

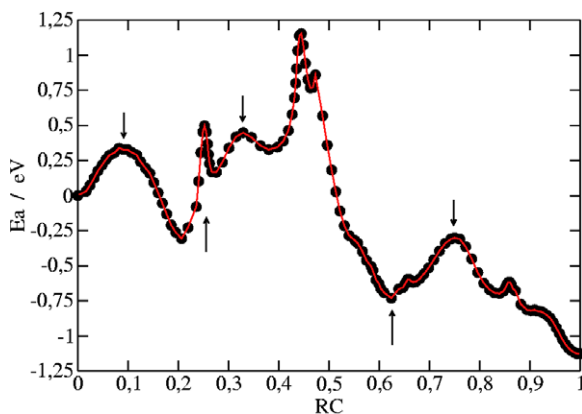


**Figure 5.** Minimum energy path for trimer exchange deposition calculated with the NEB method. The upward-pointing arrows signal the opening of the Au surface and the downward-pointing arrows show the insertion of a Co atom.

each other, with  $E_a = 0.22$  eV. However, figure 4(a) clearly shows that this final state involving the two Au atoms close to each other, as found by the quenched AD, has a higher energy than that observed by the NEB at  $RC = 0.85$ . The latter evidence reveals that the NEB procedure may also be useful to identify local minima.

The  $z$  coordinates of the atoms mainly involved in the DSE were monitored during the exchange mechanism seen in figure 4(b). As can be observed, the first Co atom is inserted with the concomitant ejection of the first Au atom. This process is different from the single Co atom deposition described above, which is in agreement with the simulation reported by Bulou [19]. The second Co atom begins to diffuse into the Au surface before the second Au atom is ejected. This generates a high compressive stress on the surface, manifest in the large surface strain around the exchange place (not shown here). Thus, the Co dimer insertion into Au(111) can be viewed as a two-step process, in which the Au second atom is expelled after the insertion of the first one is completed.

### 3.3. Trimer adatom deposition

As the size of the nuclei increases, atom dynamics simulations at 300 K become insufficient to study Co incorporation into Au, because of the increase in the waiting time for atom exchange. We have investigated the dynamic evolution of a Co trimer adsorbed on Au(111) during 50 ns at 300 K. During this period, no exchange or surface mixing was observed. However, atom dynamics simulations at 700 K showed a surface exchange process of the whole cobalt trimer. From the final configuration at 700 K, the configuration of the system was relaxed and the atomic coordinates were used as the final image for NEB calculations. A set of intermediate dynamic configurations were used as input images, since a straightforward interpolation between initial and final states was not possible.

Figure 5 shows the energy profile of the whole trimer exchange mechanism. The opening of the surface is again an activated process, marked by upward-pointing arrows in

figure 5. The first step involves a medium exchange between a cobalt atom (say,  $Co_1$ ) and two gold atoms. In this process, atom  $Co_1$  sinks into the surface, going down between the other Co atoms (say,  $Co_2$  and  $Co_3$ ) that form a bridge. At the same time, one of the Au atoms comes out of the surface at the other side of the  $Co_2$ – $Co_3$  bridge. The activation energy for this process is  $E_a = 0.33$  eV, concluding at RC near 0.2.

Subsequently, the sinking of a second Co into the surface takes place, involving the activated process observed at  $RC = 0.25$  with an  $E_a = 0.81$  eV. The insertion of the second cobalt atom ( $Co_2$ ) is an activated process with a saddle point at  $RC = 0.33$  and  $E_a = 0.27$  eV. Once this exchange occurs, a rearrangement of the first and second surface layers is related to the large activated process appearing at  $RC = 0.44$ . (See video in supplementary information (available at [stacks.iop.org/JPhysCM/20/265010](http://stacks.iop.org/JPhysCM/20/265010))). At  $RC = 0.75$  the insertion of the third cobalt atom  $Co_3$  is observed, with an activation energy  $E_a = 0.32$  eV. Finally, the rearrangement of atoms leads to the energy minimum shown at  $RC = 1$ . It must be noted that, as the number of Co adatoms increases, adatom exchange with the surface involves strongly activated processes not present in the case of single adatom insertion. For instance, in trimer deposition, the insertion of each of the three Co atoms is an activated process, whereas for a single adatom, the insertion process is practically non-activated. As stated before, the increasing difficulty in inserting Co atoms into the Au surface as the Co coverage increases bears consequences for Au surface nanostructuring with cobalt atoms, as in the case of the supersaturation-induced local metal deposition method [24].

## 4. Conclusions

The atomistic mechanism taking place during the early stages of single, dimer and trimer Co deposition on Au(111) was characterized using atom dynamics simulations coupled to the nudged elastic band method to find saddle points of the transitions.

For the insertion of the first Co atom in single, dimer and trimer nuclei, exchange with the surface is favorable against hopping surface diffusion. This exchange becomes progressively more difficult as the nucleus size increases. This is summarized in figure 6(a), where the activation energies for this process are plotted as a function of the number of cobalt atoms in the nuclei. In comparison, the activation energy for diffusion of Co on Au(111) is plotted and signaled by an arrow. Assuming first-order kinetics, if an attempt frequency of the order of 1 THz is employed to estimate the exchange times of the first Co atom, the times obtained are of the order of 0.1 ns, 1 ns and 1 s for one-, two- and three-atom nuclei, respectively. On the other hand, exchange energies for the whole nuclei suggest that this process is always favorable, as shown in figure 6(b). This plot indicates that the insertion of a set of Co atoms into Au(111) becomes progressively slower as the number of atoms in the set increases. However, the consideration of the highest energy value along the reaction coordinate in the case of the three-atom cluster would yield a waiting time of the order of  $10^9$  s for the insertion of the whole

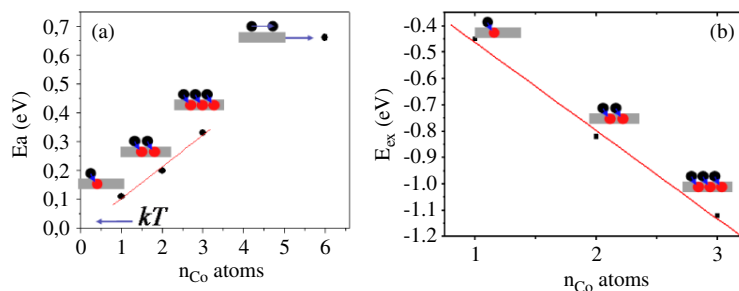


**Figure 6.** (a) Activation energies and (b) exchange energies as a function of the number of Co atoms in the nuclei. Note that the  $E_a$  value for Co diffusion on Au(111) and  $k_B T$  are marked in frame (a).

**Table 1.** Energy change for exchanging a Co atom with an Au one on an Au(111) surface.  $\Delta E_{\text{JEAM}}$  is the calculation made using the JEAM potentials.  $\Delta E_{\text{SMTB}}$  is the result obtained using the SMTB potential with the parameters of Bulou [23].  $\Delta E_{\text{DFT}}$  are first-principles calculation results with the SIESTA code [28]. The local density approximation was used for the exchange and correlation energy allowing for spin polarization. A  $(3 \times 3)$  supercell geometry was adopted, and the substrate consisted of four Au(111) layers separated by a distance of 2.1 nm. The two first surface layers were allowed to relax. The  $k$ -point sampling mesh was a  $(6 \times 6 \times 1)$  one and the energy shift was 0.01 eV.

$\Delta E_{\text{JEAM}}$ (eV)	-0.49
$\Delta E_{\text{SMTB}}$ (eV)	+0.15
$\Delta E_{\text{DFT}}$ (eV)	-2.44

nucleus in the surface, indicating that this process should not be observed within experimental timescales. The enhancement of the Co–Au site exchange in the presence of small Co clusters contrasts with previous work [23] where the diffusion of Co single atoms was found to prevail over single Co atom exchange. The main reason for this discrepancy must be sought in the nature of the interatomic potentials employed. In order to allow for further comparison, we have performed comparative calculations with the results given in table 1. We compare there the energy for exchanging a Co atom with an Au one on an Au(111) surface, according to the results obtained by the JEAM, SMTB and DFT first-principles calculations. We see that the JEAM and the DFT results lead to the same qualitative prediction, that is, that the exchange of a Co atom with an Au one on an Au(111) surface is energetically favorable. The larger absolute value obtained by DFT may be in part due to the small supercell employed and to the overbinding characteristic for LDA. This interesting controversy constitutes a motivation for further research.

This simulation also shows that an optimization of the number of participating atoms during the diffusion mechanism must be carried out. For instance, a variation from 1.20 to 0.11 eV in a typical activation energy can be obtained, depending on whether 2 or 400 atoms are relaxed in the system.

## Acknowledgments

The authors wish to thank for financial support the Consejo Nacional de Investigaciones Científicas y Técnicas (CONICET), Agencia Córdoba Ciencia, Secyt UNC, Program

BID 1728/OC-AR PICT No 946. OAO thanks CONICET for a fellowship. We wish to thank Patricio Velez for the DFT calculations.

## References

- [1] Venables J A 1997 *The Chemical Physics of Solid Surfaces* 1st edn, vol 8 (Amsterdam: Elsevier)
- [2] Labayen M, Ramirez C, Schattke W and Magnussen O M 2003 *Nat. Mater.* **2** 783
- [3] Repain V, Baudot G, Ellmer H and Rousset S 2002 *Europhys. Lett.* **58** 730
- [4] Chado I, Goyhenex C, Bolou H and Bucher J P 2004 *Phys. Rev. B* **69** 085413
- [5] Tolkes C, Zeppenfeld P, Krzyzowski M, David R and Comsa G 1997 *Surf. Sci.* **394** 170
- [6] Tolkes C, Zeppenfeld P, Krzyzowski M, David R and Comsa G 1997 *Phys. Rev. B* **55** 13932
- [7] Voigtlander B, Meyer G and Amer N 1991 *Phys. Rev. B* **44** 10354
- [8] Hofmann D, Schindler W and Kirschner J 1998 *Appl. Phys. Lett.* **73** 22
- [9] Kleinert M, Waibel H F, Engelmann G E, Martin H and Kolb D M 2001 *Electrochim. Acta* **46** 3129
- [10] Basset D W and Webber P R 1978 *Surf. Sci.* **70** 520
- [11] Feibelman P J 1990 *Phys. Rev. Lett.* **65** 729
- [12] Stumpf R and Scheffler M 1994 *Phys. Rev. Lett.* **72** 254
- [13] Stumpf R and Scheffler M 1996 *Phys. Rev. B* **53** 4958
- [14] Bogicevic A, Strömquist J and Lundqvist B I 1998 *Phys. Rev. Lett.* **81** 637
- [15] Feibelman P J and Stumpf R 1999 *Phys. Rev. B* **59** 5892
- [16] Foiles S M, Baskes M I and Daw M S 1986 *Phys. Rev. B* **33** 7986
- [17] Rosato V, Guillope M and Legrand B 1989 *Phil. Mag. A* **59** 321
- [18] Henkelman G and Jónsson H 1999 *J. Chem. Phys.* **111** 7010
- [19] Bulou H and Massobrio C 2005 *Phys. Rev. B* **72** 205427
- [20] Henkelman G and Jónsson H 2000 *J. Chem. Phys.* **113** 9978
- [21] Henkelman G, Uberuaga B P and Jónsson H 2000 *J. Chem. Phys.* **113** 9901
- [22] Bulou H, Lucas O, Kibaly M and Goyhenex C 2003 *Comput. Mater. Sci.* **27** 181
- [23] Bulou H and Massobrio C 2004 *Superlatt. Microstruct.* **36** 305
- [24] Mariscal M, Leiva E P M and Dassie S A 2007 *J. Electroanal. Chem.* **607** 10
- [25] Tildesley D J and Allen M P 1987 *Computer Simulation of Liquids* 1st edn (Oxford: Oxford University Press)
- [26] Zhou X W, Wadley H N, Johnson R A, Larson D J, Tabat N, Cerezo A, Petford-Long A K, Smith G D, Clifton P H, Martens R L and Kelly T F 2001 *Acta Mater.* **49** 4005
- [27] Johnson R A 1989 *Phys. Rev. B* **39** 12554
- [28] Gale J D, García A, Junquera J, Ordejón P, Soler J M, Artacho E and Sánchez-Portal D 2002 *J. Phys.: Condens. Matter* **14** 2745